Proceedings of the 2nd Marine Energy Technology Symposium
METS2014
April 15-18, 2014, Seattle, WA

FATIGUE LIFE DISTRIBUTION FOR A SIMPLE WAVE ENERGY CONVERTER

Adam C Brown*
NW National Marine Renewable Energy Center
Oregon State University
Corvallis, OR, USA

Robert Paasch
NW National Marine Renewable Energy Center
Oregon State University
Corvallis, OR, USA

ABSTRACT

Fatigue is known to be a dominant failure mode for systems subjected to wave loading. A time domain simulation of loading on a simple Wave Energy Converter (WEC) was used to develop the distribution of fatigue failures around the assumed 10 year design life of the device.

In order to maintain the generality of the paper, the WEC was modeled as a simple, solid, stainless steel rod under wave induced axial tension and compression. This simplified model is seen as a reasonable approximation of a hydraulic ram. The system was subjected to seas that would be typical of the Oregon wave climate. The random waves used for the analysis were generated according to linear wave theory by way of random phase reconstruction of JONSWAP spectra.

The model of the Oregon wave climate is also discussed, as it was found that the randomness within the wave climate model greatly affects the variance of the distribution of fatigue life.

An equation for stress cycle induced damage was developed according to the Linear Cumulative Damage Theorem (Miner's Rule). Time to failure and several other metrics were recorded for 300 failures in order to develop the probability distribution of fatigue life.

INTRODUCTION

Sustainable energy sources move the world around us, but the variability of these sources make them difficult to capture. Solar energy heats the water and atmosphere inducing convective flows. The wind moving across the water in turn builds waves. With each conversion, the energy becomes more dense and variable. The wind has been utilized as a power source for centuries; however, even today its variability presents a challenge to its further implementation [1–3]. Ocean wave energy is confronted by the same difficulty [4, 5]. The energy content of waves increases by the square of their height [6, §4.7]. Due to the intense loading imparted by the most energetic, yet rare waves, curtailing power production in waves above a certain height may be necessary to improve system reliability and survivability while reducing capital cost. These decisions will ultimately impact the cost of power [7]. The two main questions affecting cost of energy are: In what conditions should a WEC produce power? and How should one design for those conditions? This paper seeks to provide information that may be pertinent to understanding these questions.

Structural loading and fatigue have been widely studied for offshore systems [8–12], yet the distribution of fatigue failure around the design life of a WEC is still poorly understood. In order to develop such a distribution of fatigue life, a time domain simulation was conducted in which a WEC was modeled as a stainless steel rod being subjected to ocean wave induced axial tension and compression. Though simple, this model is expected to produce results similar to the fatigue of a hydraulic ram within the power take-off (PTO) of a WEC.

The wave spectra used for the analysis were developed from the average conditions expected off the coast of Oregon at any given point in the year (derived from data recorded by NDBC buoy 46050) [13]. The random wave-fields were then generated according to linear wave theory using random phase spectral reconstruction [14, §2.2].

An equation for system stress was derived assuming a velocity-proportional control strategy for the PTO. Load shedding techniques were not considered in this analysis. Peak stresses were then identified and the rainflow-counting algorithm was applied in order to identify stress cycles. The rainflow-counting algorithm has been well studied [15–17]. Miner's Law was assumed, and the damage associated with each of these peak stresses was counted and the accumulated damage was tracked

*Corresponding Author: brownad@onid.oregonstate.edu

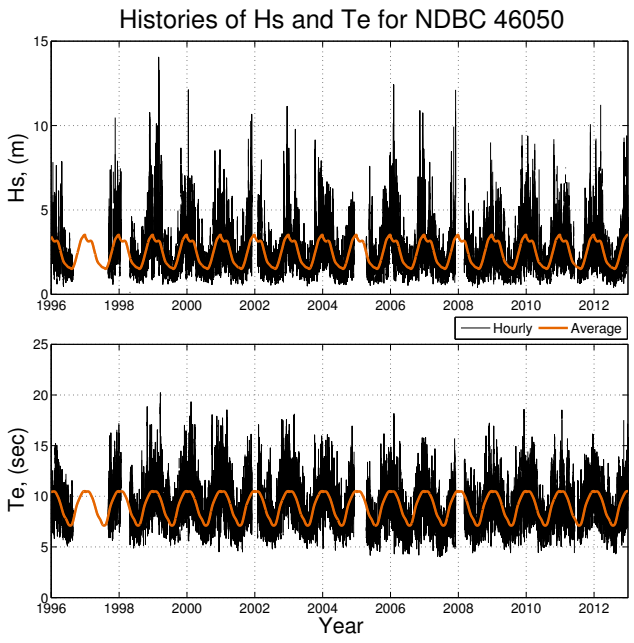

FIGURE 1. FIFTEEN YEAR HISTORY OF H_s AND T_e FOR NDBC BUOY 46050, LOCATED IN 128 m WATER DEPTH, 22 MILES OFF THE COAST OF NEWPORT, OREGON.

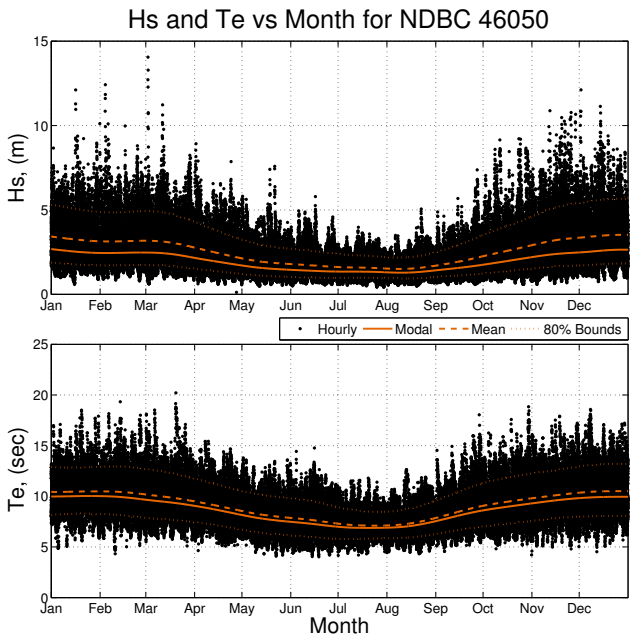

FIGURE 2. HOURLY MEAN AND MODAL H_s AND T_e FOR A GIVEN TIME OF THE YEAR. PREDICTION INTERVALS WERE DEVELOPED FROM THE DATA ASSUMING A LOG-NORMAL DISTRIBUTION.

till system failure. Details of the application of the S-N approach to fatigue analysis, and the application of Miner's Rule have been widely published and are not repeated here [18, Ch 6] [19, Ch 8]. Time to failure, stress cycles, time spent at a certain significant wave height, and the damage accumulated due to those seas were recorded.

The following sections discuss: 1) the necessary data preparation, 2) the manner by which a generic WEC was modeled, 3) the development of average yearly conditions for the mid-Oregon coast, 4) the construction of the simulation based on those average conditions, and 5) the results of that simulation.

1 Data Preparation

The data used for the analysis was acquired by the National Data Buoy Center's (NDBC) buoy number 46050 [13]. The buoy is located about 20 miles off the coast of Newport, OR in approximately 128 meters of water depth. The buoy is a discus type wave following buoy with a vertically oriented accelerometer. The buoy records the spectral energy of the ocean once per hour. Fifteen years of spectral records for this buoy are freely available and were acquired through the NDBC's website. The spectra can be used to calculate several statistical wave parameters including H_s and several measures of the wave period. The wave parameters employed in various stages of the analysis include the Significant Wave Height (H_s), the Peak Period (T_p), and the Energy Period (T_e).

As with all real data, imperfections are present. Failures of the wave-buoy or its telemetry result in missing data as can be seen in Figure 1. Even in the presence of a perfect data set, using the 15 years of data directly for the fatigue analysis would result in a lack of realistic variability, as the WEC would be subjected to nearly identical conditions every 15 years of analysis time. For these reasons, it was necessary to determine the average and variance of conditions expected during a given hour of the year. These values were calculated by overlaying the raw 15 years of data according to corresponding hour of the year. It was then assumed that a given set of wave conditions, occurring during the hour of interest would have roughly the same probability of occurrence in a 30 day time span surrounding the hour of interest. This allowed data sets to be developed for each hour of the year composed of hourly records from the 15 years of data within a 30 day period surrounding the hour of interest. The data for February 29th of the three leap years for which data was present were included in the analyzed data as additional data for February 28th. Hours during which data was not recorded were omitted from further analysis. The mean and variance of H_s, T_p, and T_e were then calculated for each hour of the year.

2 Modeling a Generic WEC

The loads examined in this study are those transmitted through the PTO and used to produce power. For this reason, the model used for the WEC can be reduced to the PTO. In an attempt to keep this study generically applicable, it was necessary to further simplify the PTO to a component that is common to most designs. Many current PTOs use a driven rod to transmit the energy of the ocean either directly to a generator, or to a hydraulic piston. For this reason, a stainless steel rod in axial tension and compression was chosen as a representative PTO component, subject to cyclic loading by the ocean environment. However, the analysis method presented here is applicable to any component within a PTO as long as a stress transfer function is known.

Rod diameter was manually adjusted such that the average time to system failure was approximately 10 years. The choice of 316 stainless steel for the rod material was made based upon the corrosive nature of the ocean environment. These choices resulted in a 3.3 cm diameter rod.

2.1 Derivation of System Load

As mentioned in the introduction, the PTO was assumed to be velocity proportional. With this assumption, it can be derived that:

$$F = C\,V\,T^3 \tag{1}$$

In this equation, F is the force imparted by the waves on the PTO. The constant, C, includes gravity, water density, and a forcing constant that is calculated based on initial assumptions for the design wave height, period, and system safety factor. The constant can be calculated by specifying a design wave of a given height and period which will produce a given power output. As we are only concerned with the peak forces on the system, V is the peak velocity of the stress cycle, and T is the period at which energy is transported by waves of a given H_s (the T_e of the wave field).

To derive Eq. 1, we start with the definition of power (P) which is force (F) times velocity (V).

$$P = FV \tag{2a}$$

We now consider the expression for the power transported by a group of waves at the group velocity (c_g), where a is the wave amplitude, ρ is the water density, and g is the gravitational constant.

$$P = \frac{\rho g}{2} a^2 c_g \tag{2b}$$

The expression for the surface elevation (η) of the water surface at a given point in space is:

$$\eta = a\cos(\sigma t) \tag{2c}$$

Taking the derivative we find that the maximum of the vertical velocity of a water particle is:

$$V = \frac{2\pi a}{T} \tag{2d}$$

Rearranging we find:

$$a = \frac{VT}{2\pi} \tag{2e}$$

In deep water:

$$c_g = \frac{c}{2} = \frac{L}{2T} \tag{2f}$$

and

$$L = \frac{gT^2}{2\pi} \tag{2g}$$

Substituting into Equation 2b and simplifying, we arrive at:

$$P = \left(\frac{\rho g}{2}\right)\left(\frac{VT}{2\pi}\right)^2\left(\frac{gT}{4\pi}\right) \tag{2h}$$

Combining all constants we find:

$$P = CV^2T^3 \tag{2i}$$

Assuming a velocity proportional control strategy we are able to substitute the definition of power into the preceding equation, and we find:

$$FV = CV^2T^3 \tag{2j}$$

At this point we put in our design wave and the desired power output from the design wave to find the value of our constant. We can then solve for force on the PTO, and arrive at Eq. 1.

2.2 Response Amplitude Operator

In calculating the motion of a WEC in response to a given wave field it is necessary to generate a RAO for heave. This process can be very complex as the true RAO is heavily tied to the geometry of the WEC. It was necessary to make significant assumptions in generating the RAO for the baseline simulation presented in this paper. The first assumption was that the buoy had some means of tuning its natural frequency (f_n) to that of the dominant wave frequency. Dynamic ballast control could be used to provide such functionality. The second assumption was that added mass was invariant. This assumption dramatically simplifies the calculation of the RAO as added mass is dependant on the geometry of the device and the frequency of oscillation. Finally, a damping coefficient (ζ) of 0.5 was assumed. This value produces buoy motion that would be typical of a WEC; yet, it is also a major assumption as the real damping coefficient will be geometry dependant, and heavily influenced by the PTO. These assumptions allow the vertical motion of the WEC (Z) to be determined by the standard transfer function for a spring-mass damper subjected to base motion [20, §3.6]. In this case, the base motion is the surface displacement of the ocean (η) and $r = f/f_n$.

$$\frac{Z}{\eta} = \sqrt{\frac{1+(2\zeta r)^2}{(1-r^2)^2+(2\zeta r)^2}} \tag{3}$$

3 The Wave Climate Model

Although each year's weather and wave conditions are unique, it is expected that the observed weather conditions will follow a similar seasonal trend from year-to-year. We will call this trend and variation around the trend the wave climate. In order to simulate unique wave conditions it was critical to accurately characterize the yearly wave climate off the coast of Newport, Oregon.

Using the data sets developed in Section 1, the wave climate was characterized by developing joint probabilities of H_s and T_p for each hour of the year. Figure 3 is presented as an example of a typical joint probability distribution for H_s and T_p. However, Figure 3 is a yearly distribution as opposed to an hourly distribution; it was unnecessary to create figures for each of the 8760 hourly joint probability distributions.

A pseudo-random number generator was developed which allowed a random number to be generated according to a given probability distribution. A pseudo-random year of H_s data could then be generated corresponding to the actual hourly probability distributions of the Oregon wave climate. Pseudo-random wave periods were generated for each hour of the year corresponding to the previously generated H_s. The result is a pseudo-random year of wave data that would be typical of the Oregon wave climate.

Based on the pseudo-random pairs of H_s and T_p which were

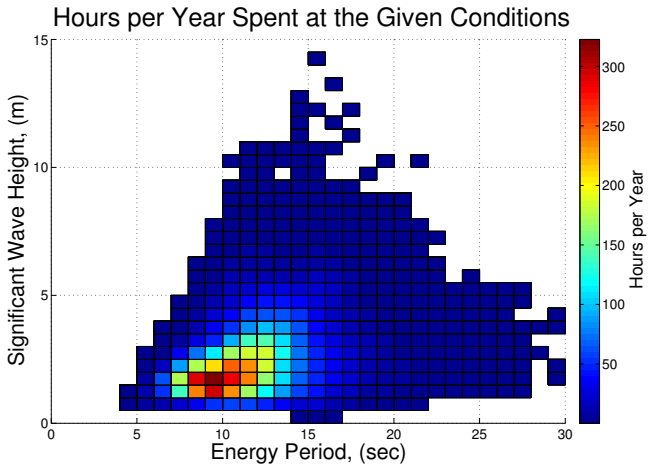

FIGURE 3. JOINT PROBABILITY OF H_s AND T_e GENERATED FROM 15 YEARS OF DATA RECORDED BY NDBC 46050 OFF THE COAST OF NEWPORT, OR.

generated for the modeled year, values of the JONSWAP peak amplification factor(γ) were determined according to the equations presented in DNV-RP-C205, and shown in Eqn. 4c [21, §3.5.5.5]. JONSWAP spectra were then generated for each set of H_s, T_p, and γ according to the following equations [22].

$$S(f) = \beta_J H_s^2 T_p^{-4} f^{-5} \exp\left[-1.25\,(T_p f)^{-4}\right] \gamma^{\exp\left[\frac{-(T_p f-1)^2}{2\sigma^2}\right]} \tag{4a}$$

where

$$\beta_J = \frac{0.0624}{0.230+0.0336\gamma-0.185\,(1.9+\gamma)^{-1}}\left[1.094-0.01915\ln\gamma\right] \tag{4b}$$

$$\gamma = \begin{cases} 5 & \text{for } \dfrac{T_p}{\sqrt{H_s}} \le 3.6 \\ \exp\left[5.75-1.15\dfrac{T_p}{\sqrt{H_s}}\right] & \text{for } 3.6 < \dfrac{T_p}{\sqrt{H_s}} < 5 \\ 1 & \text{for } 5 \le \dfrac{T_p}{\sqrt{H_s}} \end{cases} \tag{4c}$$

$$\sigma = \begin{cases} \sigma_a = 0.07 & \text{for } f \le f_p \\ \sigma_b = 0.09 & \text{for } f \ge f_p \end{cases} \tag{4d}$$

One complication inherent in wave modeling is the dependence of a given hour on the conditions of the previous hour. If

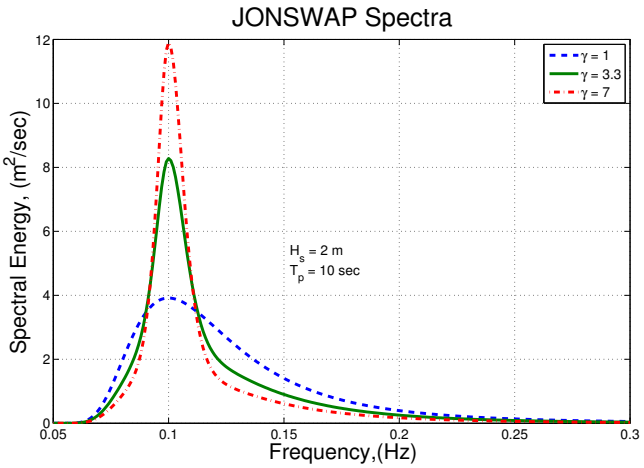

FIGURE 4. JONSWAP SPECTRA WITH CONSTANT $H_s = 2$ m, $T_p = 10$ sec AND VARYING γ.

every hour of the year were independently generated according to its own probability distribution, unrealistic discontinuities in the hour-to-hour conditions would be present in the pseudo-random year. This problem was addressed by generating data according to a single pseudo-random spectrum for a six hour period of time. Admittedly, the use of a six hour storm persistence period is imperfect; however it is simple, easy to implement, and isn't without precedence [14, §5.6.7]. Specifically, a persistence of six hours was used as it appears to be near the average duration of the peak of large storms and it is a factor of the number of hours in a year (8760 hrs per non-leap year).

4 Running the Simulation

The fatigue simulation begins after accepting the specified physical constants for the analysis: power output generated from the design wave height and period, the storm persistence period, the system damping coefficient, the time step, and the fatigue constants. As mentioned in Section 2, rod diameter was manually adjusted such that the mean fatigue life was approximately 10 years. From this information, the force constant (C) and Response Amplitude Operator (RAO) are calculated for the system. The first year of pseudo-random data is generated using the method outlined in Section 3. The buoy response amplitudes for each spectral wave component are obtained by multiplying the spectral wave amplitudes by the RAO. After the buoy response amplitudes are known the time domain analysis begins.

Due to the finite number of frequency bins used for the linear recreation of wave-fields, those wave-fields will eventually recur exactly. In order to prevent this recurrence within each six hour period, 108 independent random phase linear spectral wave-fields are developed, each of 200 second duration. The buoy response is calculated for each wave-field. The random phase spectral simulation method is well documented in the literature [23, Ch 1].

The load history is calculated according to Eqn. 1, and the peak stresses are identified. An open-source rain-flow counting algorithm was used to determine the number and amplitude of stress cycles [17]. The linear damage accumulated by each wave-field is calculated, recorded, and logged. The total accumulated damage is compared to the failure criterion which states that the system has failed if $Damage > 1$. If the system has failed, total damage is reset to zero and the simulation begins again with a new pseudo-random year at the first hour of that year. If the system has not failed, the next six hour period will begin. At the end of each year, if failure has not occurred, a new pseudo-spectral year is generated, and the simulation continues until failure.

The damage caused by each stress cycle is calculated and recorded according to the assumptions of the Linear Cumulative Damage Theorem [18, §6-8]. The equations used to determine damage ascribe a small amount of damage to even the smallest stresses; although this is counter to the concept of the endurance limit of steel, it is likely more realistic. This process was repeated for each hour of the average year, until the system was found to have failed due to fatigue. At the beginning of each new year, a new set of pseudo-random spectra were generated from the average yearly spectra and variance. The time to failure was recorded along with the hours, cycles, and damage accumulated at each H_s (hourly H_s was rounded up yielding a bin width of 1 meter). The program was stopped at 300 recorded failures. The total run time for the analysis was approximately 96 hours.

5 Results

The primary goal of this analysis was to calculate a fatigue life distribution for a WEC with a mean fatigue life of approximately 10 years. It was expected that a roughly normal distribution would exist around the design life. After 300 failures, it was in fact the case that the failure distribution developed a normal form with a mean of approximately 11.55 years and a standard deviation of 2.97 years. The failure distribution is shown in Figure 5 which includes both the Probability Density Function (PDF) as well as the Cumulative Distribution Function (CDF) of the failures.

Although the failure life distribution is fairly normal in form, there are a significant number of early life failures. This of course suggests that the devices which failed early in their life encountered very large energetic seas in those first years of operation. It may then be useful to determine the number of hours spent at a given H_s during the course of the simulation (Figure 6).

Based on Figure 6, it can be seen that wave-fields exceeding 13 meters represent less than 1000 hours of the more than 30.3 million simulated hours. Although hours of operation in seas exceeding a 13 meter H_s are rare, it may be that they contribute

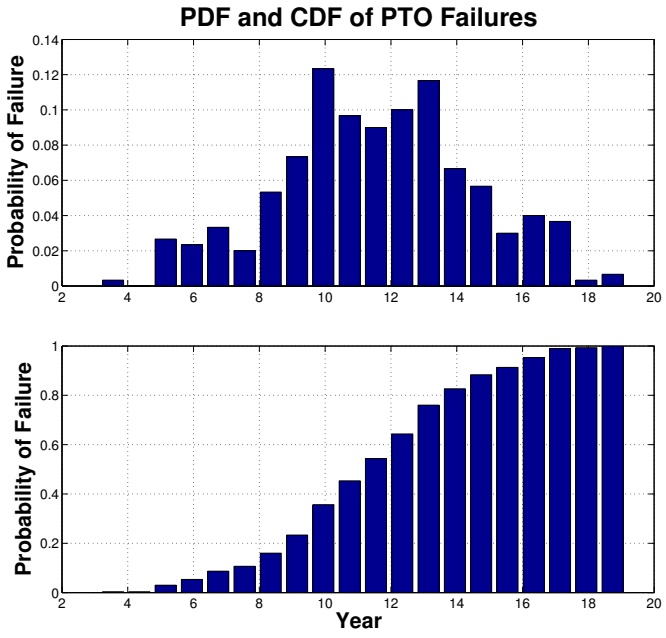

FIGURE 5. THE PDF AND CDF ARE PLOTTED FOR THE FATIGUE LIFE OF A WEC. THE MEAN FATIGUE LIFE IS APPROXIMATELY 11.5 YEARS WITH A STANDARD DEVIATION OF 3 YEARS.

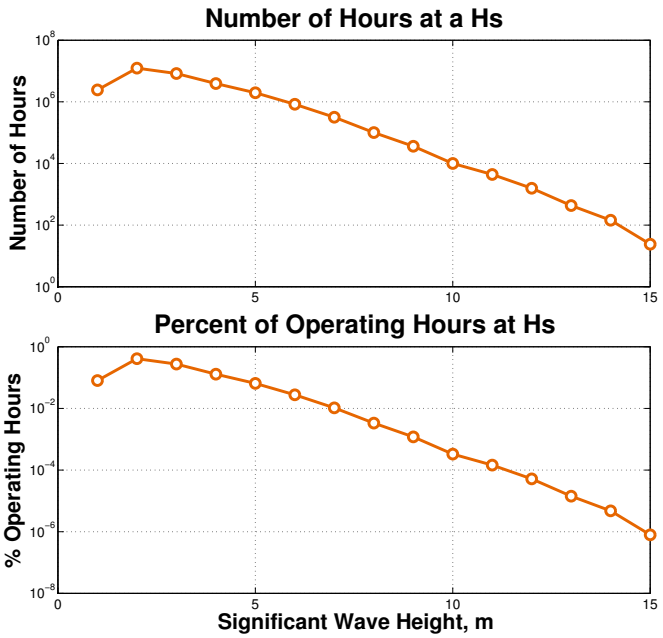

FIGURE 6. THIS IS A DUEL PLOT OF THE NUMBER OF SIMULATED HOURS AND THE PERCENTAGE OF TOTAL SIMULATED HOURS OF A GIVEN H_s. OVER 30.3 MILLION TOTAL HOURS OF OPERATION WERE SIMULATED.

significantly to the total cumulative damage of the WECs.

Figure 7 was plotted to investigate the damage that accumulated during hours of operation at each H_s. As expected seas with a H_s between 5-10 meters are responsible for the greatest percentage of system damage. However, although rare, the hours of operation in seas with a H_s greater than 10 meters contribute a significant percentage of the total accumulated damage. Specifically, it is found that 63.4% of the total damage is accumulated during hours of operation in waves with a H_s of greater than 5 meters, even though the H_s is above 5 meters only 4.3% of the time.

To clearly show the disproportionate impact of large seas on the total accumulated damage of a device, the average damage accumulated in a single hour of operation at a given H_s was plotted and is shown in the top panel of Figure 8. Miner's Rule states that when total damage reaches a value of 1, the system has failed due to fatigue. Figure 8 demonstrates that during operation in seas with a H_s of 14 meters the device will fail after being subjected to approximately 10000 stress cycles. In the context of hours of operation, seas with a H_s greater than 14 meters will cause a failure in approximately 55 hours of operation.

The endurance limit of stainless steel is reached at approximately $10^6 cycles$. Therefore, a stress resulting in damage less than 10^{-6} is a stress that is below the endurance limit of stainless

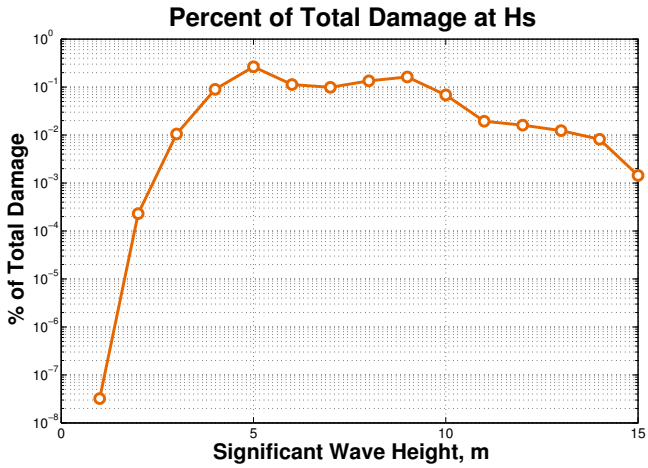

FIGURE 7. THE PERCENT OF TOTAL DAMAGE ACCUMULATED DURING OPERATION AT A GIVEN H_s IS SHOWN TO HIGHLIGHT THE CONTRIBUTION OF LARGE SEAS TO TOTAL DAMAGE.

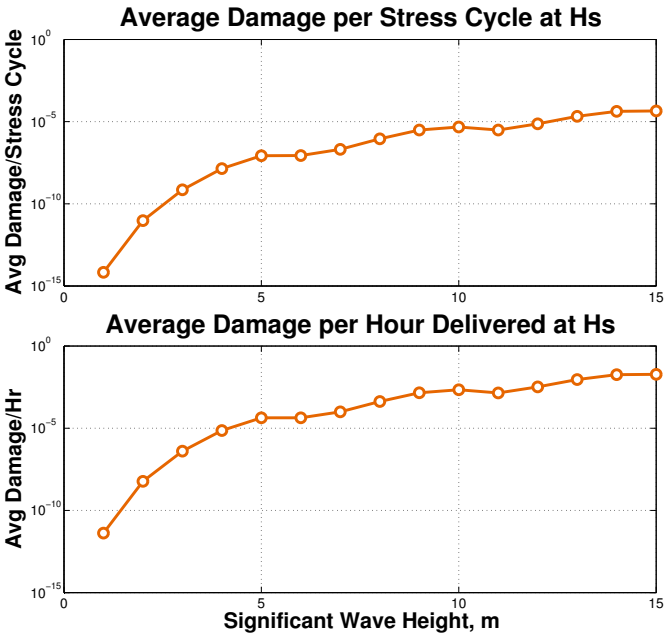

FIGURE 8. THE UPPER PANEL SHOWS THE AVERAGE DAMAGE ACCUMULATED IN A SINGLE HOUR OF OPERATION AT A GIVEN H_S. THE LOWER PANEL SHOWS THE AVERAGE DAMAGE PER STRESS CYCLE DURING OPERATION AT A GIVEN H_S.

steel. The average damage per stress cycle was also calculated and is shown in Figure 8. It can be seen that the average stress developed by a wave in seas with a H_s of 6 meters or less will be below the endurance limit of 316 stainless steel. This fact only adds emphasis to the point that extreme conditions in seas with a large H_s represent the most significant threat to a WEC both in terms of single event failures, and system fatigue.

6 Future Work

The RAO used in the analysis was developed using a damping coefficient of 0.5 along the heave axis. In reality the damping coefficient will vary depending on conditions, and depend heavily on the hydrodynamic design of the WEC. The specification of 0.5 as the damping coefficient was arbitrary, and further research will attempt to analyze the effect of damping coefficient on fatigue life.

The analysis presented in this paper was conducted in the time-domain. Individual wave-fields were developed, and the forces they would impart on a WEC PTO were then calculated. The stress developed by those forces was then analyzed to determine damage. This method is computationally intensive. By decoupling the damage calculation from the wave climate model, it may be possible to improve the fidelity of both while reducing computational time. Decoupling the damage calculation from the wave climate model would also allow for the determination of the effect of various load shedding techniques on system fatigue life.

More energy is available for extraction in large seas; however, large seas are also responsible for the majority of system damage. In order to better determine the relation of power output and system damage, it may be beneficial to record power output from the WEC during the fatigue analysis. This would allow the energy produced to be normalized by the damage accumulated resulting in a metric that could be used to determine the point at which a WEC should enter survival mode.

7 Conclusions

This paper presented the results of a time-domain simulation of system fatigue that was conducted to determine the distribution of failures around the average design life of a WEC. The WEC was designed to produce a peak of 50 kW when forced by a 2 meter, 12 second design wave. A fatigue life probability distribution was developed with a data set of 300 total failures. It was observed that early life fatigue failures accounted for a significant percentage of the total failures. This result indicates that large seas, although rare, are capable of contributing significantly to the cumulative damage of a WEC.

Through additional analysis, it was found that seas with $H_s < 5m$ induced average peak stress levels that were under the endurance limit of stainless steel. In stark contrast, it was found that over 63% of the total cumulative damage was done by seas with $H_s > 5m$ even though such seas represent only 4.3% of the total hours analyzed. This finding tends to suggest that the design wave height should be specified based on the largest seas during which power production is expected. The finding also suggests that in order to avoid system over design, load shedding techniques should be implemented.

ACKNOWLEDGMENT

This material is based upon work supported by the Department of Energy under Award Number DE-FG36-08GO18179.

Neither the United States Government nor any agency thereof, nor any of their employees, makes any warranty, expressed or implied, or assumes any legal liability or responsibility for the accuracy, completeness, or usefulness of any information, apparatus, product or process disclosed, or represents that its use would not infringe privately owned rights. Reference herein to any specific commercial product, process, or service by trade name, trademark, manufacturer, or otherwise, does not necessarily constitute or imply its endorsement, recommendation, or favoring by the United States Government or any agency thereof. The views and opinions of originators expressed herein do not

necessarily state or reflect those of the United States Government or any agency thereof.

REFERENCES

[1] Smith, J. C., Milligan, M. R., DeMeo, E. A., and Parsons, B., 2007. "Utility wind integration and operating impact state of the art". *IEEE Transactions on Power Systems,* ***22***(3), Aug., pp. 900–908.

[2] Brekken, T. K. A., Yokochi, A., von Jouanne, A., Yen, Z. Z., Hapke, H. M., and Halamay, D. A., 2010. "Optimal energy storage sizing and control for wind power applications". *IEEE Transactions on Sustainable Energy*, Jan.

[3] Halamay, D. A., Brekken, T. K. A., Simmons, A., and McArthur, S., 2011. "Reserve requirement impacts of large-scale integration of wind, solar, and ocean wave power generation". *Sustainable Energy, IEEE Transactions on,* ***2***(3), pp. 321–328.

[4] Brekken, T. K. A., von Jouanne, A., and Han, H. Y., 2009. "Ocean wave energy overview and research at oregon state university". In Power Electronics and Machines in Wind Applications, 2009, pp. 1–7.

[5] Lenee-Bluhm, P., Paasch, R., and Ozkan Haller, H. T., 2011. "Characterizing the wave energy resource of the US pacific northwest". *Renewable Energy,* ***36***(8), Aug., pp. 2106–2119.

[6] Dean, R. G., and Dalrymple, R. A., 1991. "Waves breaking in shallow water". In *Water Wave Mechanics for Engineers and Scientists*, Vol. 2 of *Advanced Series on Ocean Engineering*. World Scientific Publishing Co. Pte. Ltd., pp. 112–116.

[7] Brown, A., Paasch, R., Tumer, I. Y., Lenee-Bluhm, P., Hovland, J., von Jouanne, A., and Brekken, T., 2010. "Towards a definition and metric for the survivability of ocean wave energy converters". *ASME Conference Proceedings,* ***2010***(43949), Jan., pp. 917–927.

[8] Garbatov, Y., and Guedes Soares, C., 2001. "Cost and reliability based strategies for fatigue maintenance planning of floating structures". *Reliability Engineering & System Safety,* ***73***(3), Sept., pp. 293–301.

[9] Mansour, A. E., 1987. "Extreme value distributions of wave loads and their application to marine structures". In Proceedings of the Marine Structural Reliability Symposium, The Society of Naval Architects and Marine Engineers.

[10] Madsen, H. O., Skjong, R. K., and Tallin, A. G., 1987. "Probabilistic fatigue crack growth analysis of offshore structures, with reliability updating through inspection". In Proceedings of the Marine Structural Reliability Symposium, The Society of Naval Architects and Marine Engineers.

[11] Ayyub, B. M., Assakkaf, I. A., Kihl, D. P., and Siev, M. W., 2002. "Reliability based design guidelines for fatigue of ship structures". *Naval Engineers Journal,* ***114***(2), Apr., pp. 113–138.

[12] Ang, A. H.-S., Cheung, M. C., Shugar, T. A., and Fernie, J. D., 2001. "Reliability-based fatigue analysis and design of floating structures". *Marine Structures,* ***14***(1-2), Jan., pp. 25–36.

[13] NOAA, 2012. NDBC station page. http://www.ndbc.noaa.gov/station_page.php?station=46050.

[14] Tucker, M., and Pitt, E., 2001. *Waves in ocean engineering*. Elsevier.

[15] Matsuishi, M., and Endo, T., 1968. "Fatigue of metals subjected to varying stress". *Japan Society of Mechanical Engineers, Fukuoka, Japan*, pp. 37–40.

[16] Amzallag, C., Gerey, J. P., Robert, J. L., and Bahuaud, J., 1994. "Standardization of the rainflow counting method for fatigue analysis". *International Journal of Fatigue,* ***16***(4), June, pp. 287–293.

[17] Nieslony, A., 2012. Rainflow counting algorithm. http://www.mathworks.com/matlabcentral/fileexchange/3026-rainflow-counting-algorithm.

[18] Budynas, R., and Nisbett, K., 2010. *Shigley's Mechanical Engineering Design*, 9 ed. McGraw-Hill Science/Engineering/Math, Jan.

[19] Juvinall, R. C., and Marshek, K. M., 2000. *Fundamentals of Machine Component Design*, 3 ed. Wiley.

[20] Rao, S. S., 2003. *Mechanical Vibrations*, 4 ed. Pearson Education India.

[21] Det Norske Veritas, 2010. Environmental conditions and environmental loads. Standard DNV-RP-C205, Det Norske Veritas, Oct.

[22] Gōda, Y., 2010. *Random seas and design of maritime structures*. World Scientific, June.

[23] Kim, C. H., 2008. *Nonlinear Waves and Offshore Structures*. World Scientific.